ACS SENSORS

Article

Cite This: ACS Sens. 2019, 4, 1662−1669

pubs.acs.org/acssensors

Cellulose Fibers Enable Near-Zero-Cost Electrical Sensing of Water-Soluble Gases

Giandrin Barandun,[†] Matteo Soprani,[†,‡,§] Sina Naficy,[†,∥] Max Grell,[†] Michael Kasimatis,[†] Kwan Lun Chiu,[†] Andrea Ponzoni,[‡,§] and Firat Güder*[,†]

[†]Department of Bioengineering, Imperial College London SW7 2AZ, London, United Kingdom

[‡]Department of Information Engineering University of Brescia 25123, Brescia, Italy

[§]National Institute of Optics National Research Council 25123, Brescia, Italy

[∥]School of Chemical and Biomolecular Engineering The University of Sydney NSW 2006, Sydney, Australia

Supporting Information

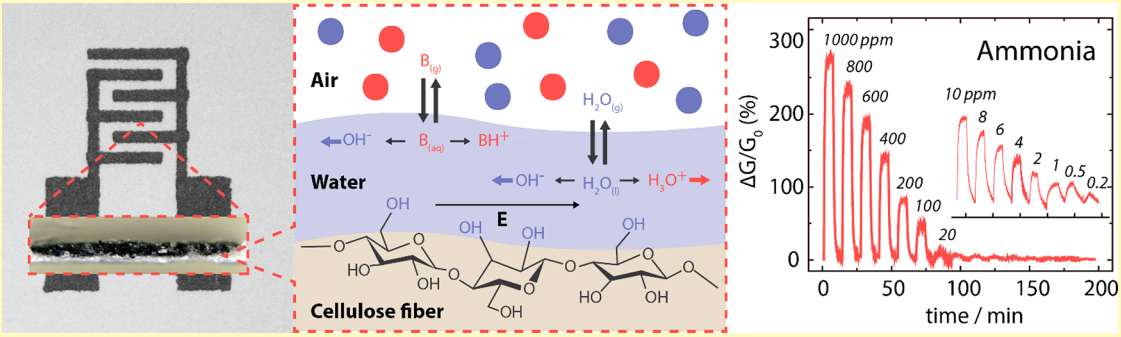

ABSTRACT: We report an entirely new class of printed electrical gas sensors that are produced at near "zero cost". This technology exploits the intrinsic hygroscopic properties of cellulose fibers within paper; although it feels and looks dry, paper contains substantial amount of moisture, adsorbed from the environment, enabling the use of wet chemical methods for sensing without manually adding water to the substrate. The sensors exhibit high sensitivity to water-soluble gases (e.g., lower limit of detection for NH_3 < 200 parts-per-billion) with a fast and reversible response. The sensors show comparable or better performance (especially at high relative humidity) than most commercial ammonia sensors at a fraction of their price (<$0.02 per sensor). We demonstrate that the sensors proposed can be integrated into food packaging to monitor freshness (to reduce food waste and plastic pollution) or implemented into near-field-communication tags to function as wireless, battery-less gas sensors that can be interrogated with smartphones.

KEYWORDS: *Sensors, cellulose paper, waste prevention, food quality, RFID tags*

Food waste is a major global problem with substantial economic and environmental consequences;[1] 30% of all food produced for human consumption (∼1.3 billion tons) is thrown away each year.[2] Although this number arises from various inefficiencies throughout the entire supply chain, food waste by consumers is a major contributor.[3] In the United Kingdom, for instance, food waste by households amounts to 7 million tons every year, 60% of which (4.2 million tons, worth $12.5 billion) is estimated to be safe to consume, yet discarded by consumers.[4]

The freshness of packaged foods is estimated by the use-by date that appears on the packaging. The use-by date is an approximation for the date on which a perishable product may no longer be edible. However, this does not reflect the actual state of freshness of the consumable, because it is dependent on, in addition to formulation and packaging, the storage and processing conditions.[5] More than one third of consumers throw away food solely because it is close to (or passed) the use-by date, regardless of its actual freshness. Inefficient consumption of food produces significant plastic pollution. This is another dimension to the issue of discarding food prematurely that has catastrophic environmental consequences, yet it is often overlooked.[6]

A more precise alternative to the use-by dates is the integration of disposable sensors in the packaging (this concept is known as intelligent/smart packaging).[7−10] Sensors can help monitor the state of perishable foods and communicate their condition to the user in real time. Such technologies range from relatively simple and qualitative temperature−time indicators to sophisticated and quantitative chemical monitors that measure the decomposition gases in packaged foods.[11−17] Despite the overwhelming advantages of smart packaging,

Received: March 21, 2019
Accepted: May 8, 2019
Published: May 8, 2019

DOI: 10.1021/acssensors.9b00555
ACS Sens. 2019, 4, 1662−1669

retailers and manufacturers are not willing to include freshness sensors into the food packaging for four reasons:[18]

(i) The existing solutions are not commercially viable, because they increase the cost of packaging by more than 100%.

(ii) Integration of sensors into packaging requires complex fabrication processes.

(iii) Most low-cost solutions are colorimetric indicators that are subjective (not everyone sees colors the same), difficult to use, and, at best, semiquantitative.

(iv) Existing solutions are not fully compatible with digital platforms—i.e., the output generated is not electrical and/or cannot be digitized easily.

To be commercially viable, a spoilage sensor must be nondestructive, easy to use, flexible (most packaging has curved surfaces), compatible with packaging technologies, and most importantly, ultra low cost (practically zero cost). Furthermore, the sensor should ideally be biodegradable or contain only nontoxic materials (no metals, semiconductors, etc.) to prevent contamination of food and reduce/eliminate environmental impact.[19]

We propose a highly sensitive, eco-friendly, near-zero-cost, paper-based, electrical gas sensor (PEGS) technology for the sensing of water-soluble gases such as ammonia, trimethylamine, carbon dioxide, etc. at room temperature (i.e., without heating). Paper is often used as a carrier substrate for other materials, such as carbon nanotubes, to detect gases.[20] However, our approach for sensing gases is entirely different to the existing methods; we exploit the intrinsic hygroscopic characteristics of cellulose paper to create a truly low-cost device. Highly hygroscopic cellulose fibers within paper contain a substantial amount of moisture adsorbed on their surface from the environment. Although cellulose paper feels and looks dry, it is always wet. In fact, at a relative humidity (RH) of 50%, paper contains ∼5% water by weight (water content of paper varies with RH; see Figure S1 in the Supporting Information (SI)). This phenomenon enables the use of wet chemical methods for the sensing of water-soluble gases.[21,22] The electrical properties of the thin film of water adsorbed on the cellulose fibers within paper can be probed by measuring the electrical impedance (or simply conductance) of paper using two graphite electrodes printed on the surface of paper. When a water-soluble gas is present in the immediate surrounding of paper, it increases the ionic conductance of paper. These additional ions come from the dissociation of water-soluble gases in the surface-bound thin film of water.

We have applied the PEGS technology to quantitatively monitor the freshness of packaged foods through sensing of spoilage gases, primarily focusing on meat products such as fish and poultry. We have cross-validated the results obtained from PEGS for monitoring spoilage with conventional microbiological testing (i.e., bacterial cultures). Finally, we demonstrated that the sensors produced can be integrated into near-field communication (NFC) tags to function as on/off-type disposal sensing devices for detecting gases wirelessly from within packaging, using a smartphone.

Sensor Fabrication. We fabricated the PEGS by printing interdigitated carbon electrodes on Whatman Chromatography 1 cellulose paper (manufactured by General Electric Healthcare), using a ballpoint pen and a cutter plotter (Figure 1A). We used a commercial carbon ink, which was diluted with a propriety solvent (both materials sourced from Gwent

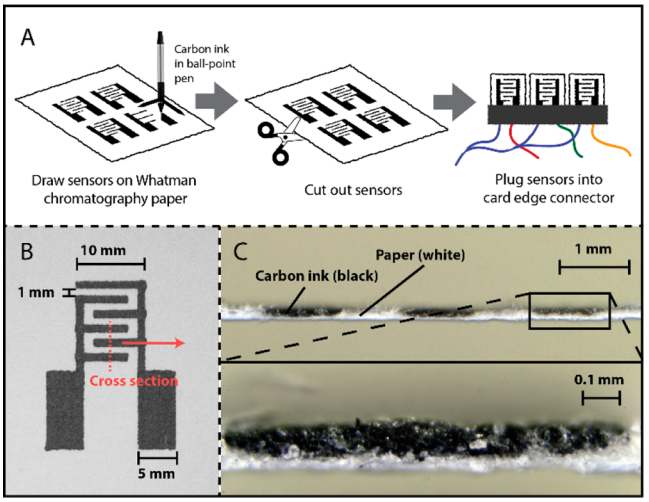

Figure 1. (A) Fabrication of paper-based electrical gas sensors (PEGS). Carbon electrodes are printed on Whatman Chromatography 1 cellulose paper with a ballpoint pen and cutter plotter, allowing rapid prototyping in the desired geometry. Once printed, the sensors are cut and placed inside a card-edge connector for characterization. (B) Top view of a single PEGS consisting of two electrodes with three fingers and a spacing of 1 mm between each finger. (C) Cross-sectional view of a PEGS across three fingers (red dashed line in panel (B)). Carbon ink (black) partially penetrates paper (white).

Electronic Materials, UK) with an ink-to-solvent ratio of 55:45 by weight, to improve printability. This method of fabrication allows for rapid prototyping and precise digital adjustment of various design parameters—e.g. surface area, size, number of interdigitated fingers, and the amount of ink deposited to tailor performance characteristics. Figures 1B and 1C show top and cross-sectional optical images of the sensors produced. Surface areas of the interdigitated electrodes, and the spacing between them, are the main factors determining the overall impedance of the sensors, which have a critical effect on its sensitivity. We used a transimpedance amplifier (Figure S2 in the SI) to convert the electrical output of PEGS (the current running through the sensor) to a voltage signal to enable digitization of the analog signal, using an analog-to-digital converter (ADC) on a microcontroller. When the base impedance of the paper sensor is high, the current running through the sensor is low; therefore, the signal must be amplified, which, in turn, results in higher sensitivity to gases since the absolute electrical contribution to ionic conductivity by a gas is the same whether the sensor has a lower or higher base impedance (see the section entitled "Modeling of Sensing Mechanism", presented later in this work). On the other hand, there are limitations to the maximum impedance that can be used for sensing, because it becomes increasingly difficult to build low-cost electronics for signal amplification without a decrease in signal-to-noise ratio. Hence, a degree of optimization is required to produce a sensitive, yet cost-effective system.

The carbon electrodes printed on paper had a typical resistance of 6.40 ± 2.75 kΩ/□ (n = 7). This is several orders of magnitude lower than the impedance of paper (10 MΩ to several GΩ); therefore, the contribution of the electrode resistance to the overall impedance of paper is negligible. Throughout the experiments, we did not alter the electrical characteristics of the carbon electrodes, but, nevertheless, the

DOI: 10.1021/acssensors.9b00555
ACS Sens. 2019, 4, 1662−1669

resistance of the electrodes can be modified using multiple passes of the ballpoint pen.

RESULTS AND DISCUSSION

Sensor Characterization. We measured the impedance of paper between the interdigitated electrodes to determine the conductance of PEGS when exposed to water-soluble gases. All calibration experiments were performed after flushing the sensors in the test chamber with humidified nitrogen for at least 1 h. We tested the sensors against ammonia (NH_3), trimethylamine (TMA), hydrogen sulfide (H_2S), carbon dioxide (CO_2), and carbon monoxide (CO). Each test gas, diluted in high purity N_2 to a known concentration by the supplier, was purchased from the BOC Group PLC and further mixed with humidified and dry nitrogen at different ratios to adjust RH (35%−95%) and concentration ($0.2-10^6$ parts-per-million [ppm]) to the level desired for the experiments. To measure the response of the sensors to a target gas, we applied sinusoidal excitation at various frequencies ($10-10^3$ Hz) and amplitudes (0.1−10 V) as the input signal. We calculated the conductance (G) of the sensor using Ohm's law by dividing the current passing through the sensor by the applied potential. We determined the baseline conductance of PEGS at the set RH levels when no test gas was present, e.g., in pure (humidified) nitrogen atmosphere (G_0). Using G and G_0, we calculated the change in conductance of paper sensors ($\Delta G/G_0$) in response to the test gas.

The PEGS exhibited a high intrinsic selectivity toward ammonia, compared to the other gases tested (TMA, H_2S, CO_2, CO) (see Figure 2A). PEGS were more than 20 times more sensitive to NH_3, compared to TMA and CO_2, while both CO (below 10^3 ppm) and H_2S (below 10^4 ppm) were undetectable by the sensors. Figure 2B shows the response of the sensor ($\Delta G/G_0$) when exposed to a wide range of ammonia concentrations (0.2−1000 ppm). The change in conductance was proportional to the ammonia concentration, with a lower limit of detection of ~0.2 ppm (Figure 2C) at ~70% RH. Note that the threshold for the detection of ammonia by the human nose is ~50 ppm, although this may be dependent on the individual.[23,24] The response of PEGS for ammonia can be approximated by two separate linear regions across the lower (0.2−2 ppm) and higher ($2-10^3$ ppm) range of concentrations (Figure S3 in the SI). The sensors were more sensitive to ammonia in the range of 0.2−2 ppm than $2-10^3$ ppm, as indicated by the slopes of the fitted (linear) lines (0.24 vs 1.1), probably because of the change in concentration of ionic species due to increasing pH.[25]

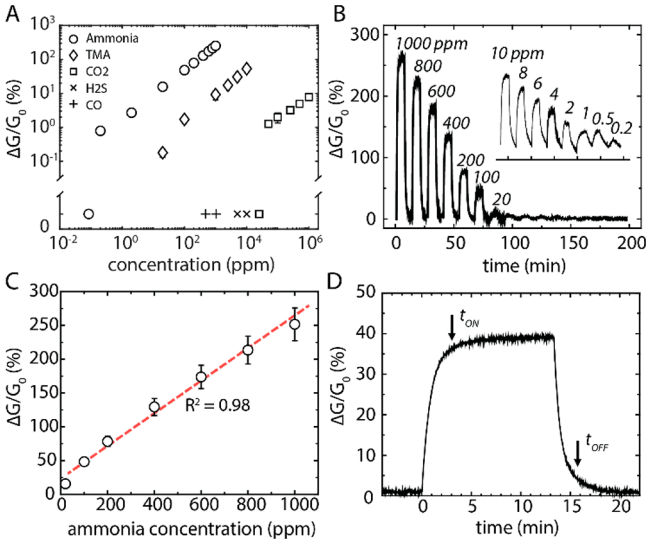

Figure 2. (A) Response of PEGS to ammonia (○), TMA (◇), CO_2 (□), H_2S (×), and CO (+). Error bars indicate standard deviation for n = 5 but may not be visible due to low variation. All experiments were performed at 70% RH. (B) Response of PEGS to varying concentrations of ammonia in the range from 0.2 ppm to 1000 ppm with exposure and purge times of 400 s. (C) The average electrical response of PEGS (n = 6) as a function of ammonia concentration. (D) Electrical response of PEGS to 80 ppm of ammonia with arrows indicating $t_{ON/OFF}$ values for 90% of the target level.

Regardless of the ammonia concentration, the sensors reached their final decile of $\Delta G/G_0$ within 186 ± 7 s (t_{ON}, n = 5). Immediately after ammonia was replaced by pure nitrogen, G decreased to 10% of its original peak value within 163 ± 9 s (t_{OFF}, n = 5). Both t_{ON} and t_{OFF} values were similar to those of commercially available electrochemical ammonia sensors such as the EUROGAS 4-NH3-100 ammonia sensor, with a $t_{ON/OFF}$ value of <90 s (Figure 2D). We investigated the impact of environmental (e.g., temperature and RH) and operational (e.g., amplitude and frequency) parameters on the response of the sensors. At different temperatures within the range of 20−30 °C and at 60% RH, we exposed the sensors to 5 ppm ammonia (Figure 3A). In this range, the temperature shows no effect on the response of the sensors. However, the temperature does have an influence on gas solubility and ionic mobility in solution. Therefore, we assume that the effect in

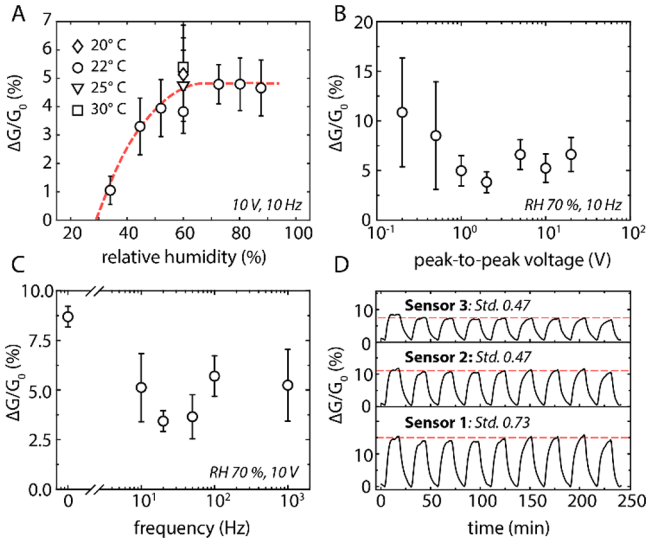

Figure 3. (A) Average electrical response of PEGS (n = 6) to 5 ppm ammonia, as a function of RH. For 60% RH, we tested at different temperatures (20−30 °C). (B) Impact of peak-to-peak voltage of the sinusoidal potential applied to the interdigitated electrodes, and the response of PEGS (n = 6) to 5 ppm ammonia. (C) Sensor response (n = 6) to 5 ppm ammonia with different frequencies of the applied sinusoidal potential. The data point at 0 Hz frequency shows the sensor behavior with a DC signal applied. Error bars indicate standard deviation in subplots A−C. (D) The response of PEGS to 10 ppm of NH_3 for three sensors over nine consecutive exposure cycles (800 s) at 78% RH. The average response of each sensor is shown as a dashed line, along with the standard deviation. When averaged over all cycles for all three sensors, the mean of the peak response is 10.71%, with a standard deviation of 3.37% (n = 27).

DOI: 10.1021/acssensors.9b00555
ACS Sens. 2019, 4, 1662−1669

the temperature range tested is small and lies within the error bars. RH had a positive impact on sensitivity; for instance, when exposed to 5 ppm ammonia (10 V, 10 Hz), the sensor response ($\Delta G/G_0$) increased from 1% for RH ≈ 37% to ~4% at RH ≈ 60%. For RH above 60%, no further change in $\Delta G/G_0$ was observed (Figure 3A). It has been suggested that the water adsorbed in paper exists in three different states, depending on the RH value.[26] At low RH (<30%), water forms a strongly bound monolayer around the cellulose fibers. As the RH value increases (30%−70%), more water is adsorbed on the surface of the fibers, increasing the amount of water that is less strongly bound to the surface. At RH > 70%, water is mainly present as free water in paper, which essentially behaves as bulk water. This agrees with the observed behavior that, at high RH (>60%), no further change in $\Delta G/G_0$ is detected. In addition, increasing RH reduces the base impedance and produces a better signal-to-noise ratio, improving signal quality and hence sensitivity. In contrast, the resistivity of paper decreases exponentially with RH, which negatively impacts the performance of PEGS (see Figure S4 in the SI).

Between the two operational factors we studied, the amplitude of the voltage applied (0.1−10 V, Figure 3B) had a larger impact on the quality (sensitivity and standard deviation) of the output signal than the input signal frequency ($10-10^3$ Hz; see Figure 3C). This was expected, since frequency dependence of ionic conductivity (the Debye−Falkenhagen effect) is negligible in this frequency range.[27]

At any given RH, the PEGS produced a stable and repeatable electrical response to ammonia (Figure 3D). We tested three separate sensors, where each was subjected to nine consecutive cycles of ammonia (78% RH, 10 ppm ammonia, 800 s intervals, 3.3 V, 10 Hz) followed by nitrogen to remove ammonia from the test chamber. Figure 3D shows the output of the sensors in which the dashed line indicates the average peak reading for each sensor. For a total of 27 samples (3 sensors, 9 cycles of gas exposure each), we achieved an average of 10.71% ± 3.37% standard deviation. Individual sensors had a standard deviation of 0.47%−0.73%. The coefficient of variation (COV)[28] is <0.07 for individual sensors and 0.32 for different sensors, which is within the acceptable range for commercial applications (e.g., the EURO-GAS 4-NH3-100 ammonia sensor has a COV of 0.26, the FIGARO TGS 826 MOS ammonia sensor has a COV of 0.27; these values were obtained from the datasheets).

Modeling of Sensing Mechanism. When a water-soluble gas such as ammonia ($X_{(g)}$) is introduced to the atmosphere of paper, it will partly dissolve ($X_{(aq)}$) in the thin layer of water present on the cellulose fibers within paper. Figure 4 illustrates the sensing mechanism for an alkaline gas schematically, as an example. Depending on the nature of the gas dissolved, further acidic or basic dissociation reactions may occur, resulting in various charged species (X^-/X^+, H_3O^+/OH^-):

$$X_{(aq)} + H_2O \rightarrow \cdots \rightarrow X^- + H_3O^+ (\text{acidic})$$

$$X_{(aq)} + H_2O \rightarrow \cdots \rightarrow X^+ + OH^- (\text{alkaline})$$

X^- and X^+ represent the negatively and positively charged ions generated by the reactions between the dissolved gas ($X_{(aq)}$) and water. The additional ions produced because of the gas water reaction impact the ionic conductivity of paper. The amount of the impact is dependent on the concentration of

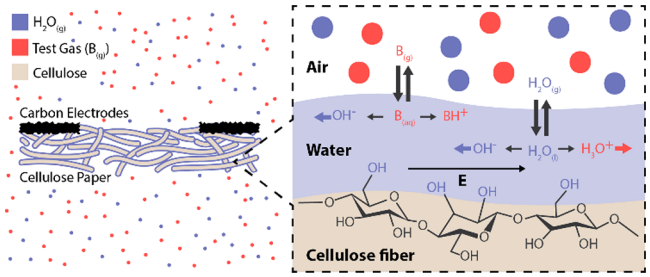

Figure 4. Model of the sensing mechanism for an alkaline test gas ($B_{(g)}$). The interconnected network of cellulose fibers within paper is covered with a thin film of water (left). The water in the paper is in equilibrium with the relative humidity (RH) and any gas present. Reacting with water, the dissolved gas ($B_{(aq)}$) dissociates to generate cations (BH^+) and hydroxide anions (OH^-). The generation of additional ions directly impacts the ionic conductivity, which is measured by applying an external potential (E) across paper, using two carbon electrodes and measuring the ionic current.

$X_{(g)}$ in the surrounding, immediate atmosphere. The increase in conductivity (σ) due to dissociation of the target gas is dependent on the ionic mobility (u_{ion}), charge (Z_e), and concentration of ions (n_{ion}):

$$\sigma = n_{ion} \times Z_e \times u_{ion}$$

These parameters are determined by the nature of the target gas (solubility (δ_H), dissociation constant (K_d), and mobility (u), in water) and the partial pressure of the gas, p_X, which is directly related to the concentration of the gas in the atmosphere. At constant RH and temperature, the amount of water adsorbed in paper remains constant; hence, any change in impedance is caused only by the variation in the concentration of gas in the surrounding atmosphere. Based on our results, we propose that the concentration of ammonia in atmosphere, for example, can be determined by measuring the elevated ionic conductivity due to the additional ammonium (NH_4^+) and hydroxide (OH^-) ions generated from the dissociation of ammonia in water:

$$NH_{3(g)} \leftrightarrow NH_{3(aq)}$$

$$NH_{3(aq)} + H_2O \leftrightarrow {NH_4}^+{}_{(aq)} + {OH}^-{}_{(aq)}$$

Ammonia has one of the highest Henry's law solubility constants (k_H^θ) of all gases (k_H^θ = 67.75 ± 10.90 mol/(kg bar) at 25 °C), with an equilibrium water reaction constant of 1.79 × 10^{-5} at 25 °C.[29] Therefore, minute amounts of ammonia in the atmosphere can substantially elevate ionic concentrations, which can be detected through electrical impedance measurements.

The lower sensitivity of the PEGS to other water-soluble gases such as CO_2, CO, H_2S, or TMA is explained by their different levels of dissociation, solubility, and ion mobility in water. Both NH_3 and TMA are nitrogenous bases and are readily protonated to generate ammonium and trimethylammonium cations. In contrast, CO_2 and H_2S are acidic, and, in water, they dissociate to generate anionic species. CO does not react with water at room temperature. The aqueous solubility and dissociation constants of TMA, CO, CO_2, and H_2S are significantly lower than ammonia in water (see Table S1 in the SI). Among the gases we tested, ammonia has the highest water solubility followed by TMA, while the solubilities of H_2S, CO, and CO_2 are ~2000 times lower. For example, 0.2 ppm

DOI: 10.1021/acssensors.9b00555
ACS Sens. 2019, 4, 1662−1669

gaseous ammonia ($NH_{3(g)}$) yields a 2.8 mM ammonia solution, if in contact with bulk water.[30] This solution will contain 0.2 mM of solvated (neutral) ammonia ($NH_{3(aq)}$) and 2.6 mM ammonium (NH_4^+) at pH 8. At this ionic concentration, the ionic conductivity of water increases by ~3 orders of magnitude, from $\sim 10^{-7}$ S cm^{-1} to 10^{-4} S cm^{-1}. This 1000-fold increase in conductivity is detectable by the PEGS. CO_2, on the other hand, has a low solubility in water, meaning that even at a concentration of 10 000 ppm, the concentration of bicarbonate (HCO_3^-) in water is only $\sim 4.4 \times 10^{-5}$ mM. Such low ionic concentrations do not produce a measurable signal. The calculations based on the solubility, dissociation, and mobility of a gaseous analyte and its ions provide a sufficiently accurate model to estimate (within 1 order of magnitude) the response of the sensor to a target gas. Generally, however, more factors may be included to allow for more accurate predictions (for further discussions on the accuracy of the model presented, please see section SI–P1 in the SI).

Quantitative Monitoring of Food Spoilage. We used PEGS to nondestructively monitor spoilage of meat products (fish and poultry) and cross-validated the results with conventional microbiological cultures to demonstrate the suitability of PEGS in smart packaging. When monitoring the decomposition of fresh meats, PEGS act as a sensor of total-volatile-basic-nitrogen (TVB-N). Ample amounts of TVB-N are produced when meat products decay. Because of this, TVB-N testing may be used as an index to assess the quality of meat products, including fish.[31] The main components of TVB-N are NH_3 and the related TMA and DMA (dimethylamine), where three or two of the H atoms of ammonia are substituted by methyl groups, respectively. In contact with water, all three gases behave similarly: First, they partly dissolve in water, according to Henry's law,[32] then dissociate into ions and change the ionic strength of the solution. By measuring the ionic strength of the solution, it is possible to determine the level of TVB-N and estimate the freshness of meat. Some attempts have been made to exploit this concept for developing food sensors; yet, the prototypes that have been developed thus far are cumbersome, expensive, and not compatible with flexible packaging and industrial manufacturing processes.[33]

As shown above, PEGS can sensitively detect ammonia and TMA (and probably DMA, although we did not test it), which are two of the most important gases involved in the decomposition of food of animal origin. Although the ionic conductivity of paper changes with both varying levels of RH and water-soluble gases, the RH inside a package of fresh meat reaches equilibrium and remains constant at ~100% RH. Hence, any increase in conductance of paper is due to the decomposition gases and not the RH, since the RH value is constant. To accelerate reaching equilibrium with the ~100% RH inside packaging, we added 20 μL of deionized (DI) water to each PEGS (see the Experimental Section for more information). We placed a total of 12 paper sensors in six separate sealed plastic boxes (two sensors per box), each with a volume of 180 mL, to monitor microbial spoilage of fish and poultry: the first two boxes contained 40 g fillets of cod, the second set of two boxes contained lean chicken breast (20 g), and the last set of two boxes contained DI water as a control (see Figure S5 in the Supporting Information). Using our custom electronics, we simultaneously recorded the impedance of each sensor placed inside the boxes at room temperature (potential applied: sinusoidal, 10 V, 10 Hz). We normalized the signal response to relative change in percentage per 100 g of fish/chicken ($\Delta G/G_0$ [100 g]$^{-1}$). This allows comparison between different amounts of meat. The PEGS in the box containing only DI water showed little to no change in their response throughout the entire duration of the experiment. In comparison to the control experiment with only DI water, the PEGS in the containers with fish and poultry exhibited a >900% increase in sensor response over the course of the experiments (see Figures 5A and 5B). This increase is due to

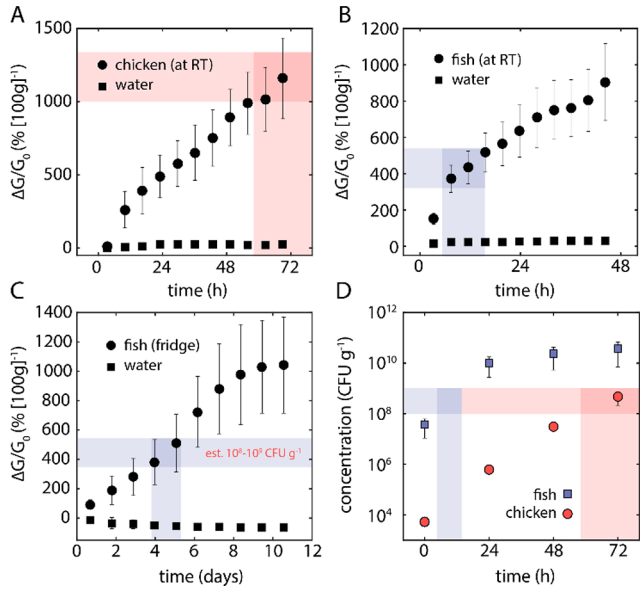

Figure 5. Monitoring gases in the headspace of spoiling fish and chicken with PEGS and cross-validation with microbial cultures. The sensor response is normalized to 100 g of meat. (A) Response of PEGS (n = 4) to decaying chicken breast at room temperature and water as control (n = 2) over 72 h. The colored bands correspond to the healthy limit of microbial contamination which was determined by microbial cultures shown in graph D. (B) Response of PEGS (n = 4) to decaying fillet of cod at room temperature and water as control (n = 2) over 50 h. The colored bands correspond to the healthy limit of microbial contamination which was determined by microbial cultures shown in graph D. (C) Response of PEGS (n = 4) to decaying fillet of cod and water as control (n = 2), both at 4 °C, over 12 days. The colored bands correspond to the healthy limit of microbial contamination which was determined by microbial cultures shown in graph D. Using this approach, a use-by date was estimated to be ~4–5 days after purchase. (D) Bacterial counts for the meats monitored at room temperature. A count of 10^8–10^9 colony-forming units per gram (cfu g^{-1}) corresponds to a limit of healthy consumption.

the gases released by the decaying meat. To monitor spoilage gases at a lower storage temperature (4 °C), we placed three containers (two with a 35 g fillet of cod and two sensors in each container, and another containing DI water and two sensors as control) inside a household refrigerator (Beko, Model LSG1545) and used PEGS to measure the change in conductance over 10 days (Figure 5C). Over the course of the 10-day experiment, while the response of PEGS in the container with DI water remained steady around the baseline, the response of PEGS in the containers with cod increased by more than 1000%. This indicates that the sensors can detect decomposition at both room and lower temperatures.

We have cross-validated the increasing electrical response, produced by PEGS due to spoilage, with microbiological assays

DOI: 10.1021/acssensors.9b00555
ACS Sens. 2019, 4, 1662–1669

every 24 h (Figure 5D).[34] The critical threshold of bacterial concentration at which most categories of food is considered spoiled, is around 10^8–10^9 CFU g^{-1} (colony-forming units per gram).[35] From the microbiological data, we approximated the critical time (t_c) at which the microbial count (normalized per mass) exceeded 10^8–10^9 CFU g^{-1}. At room temperature, for samples of fish, t_c was ∼10 h while for chicken breast, t_c was 70 h (shaded bands in Figure 5D). We correlated the readings from PEGS to t_c for fish and chicken and estimated a threshold for safe consumption in terms of $\Delta G/G_0$ $[100\ g]^{-1}$. While the threshold for fish was ∼400%, it was 1200% for chicken (shaded bands in Figures 5A and 5B). Because the sensor's response does not change significantly with temperature (see Figure 3A), we used the 400% threshold value for fish obtained through experiments at room temperature to estimate that the product would no longer be safe for consumption after 4–5 days when stored at 4 °C in the refrigerator (Figure 5C). For the fresh fish product used in this carefully designed experiment, the use-by date issued by the manufacturer was also consistent with our experimental results. Please see section SI–P2 and Figure S6 in the SI for more details on the analysis of the spoilage data.

Integration of Paper Sensors in NFC Tags. To realize on/off-type low-cost wireless gas sensors that can be interrogated using a smartphone, we integrated PEGS into a commercial NFC tag. We bypassed the silicon-based integrated circuit (IC) on the tag with a resistor and a PEGS (Figure 6).[36]

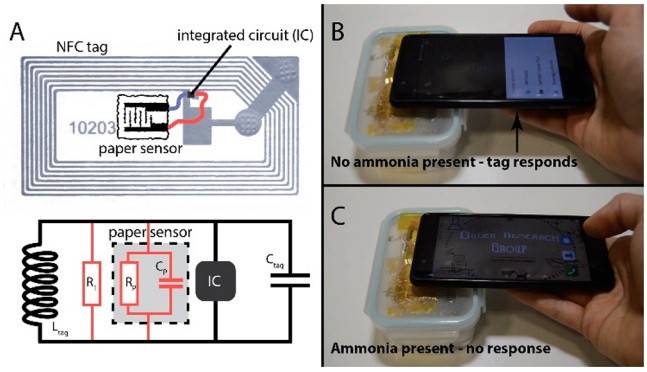

Figure 6. (A) Schematic illustration of an NFC tag (top) modified with a PEGS that bypasses the integrated circuit (IC) attached to the tag. In the circuit diagram (bottom), the original circuit components (IC), a capacitor (C_{tag}) and the antenna (L_{tag}) are shown in black. Our modifications are highlighted in red: resistor (R_1) and a PEGS with resistance R_p and capacitance C_p. The modifications disrupt communication between the reader and tag once a certain amount of gas (in this case, ammonia) is present. The resistor R_1 is used to adjust the concentration threshold at which the tag stops working. (B) Photograph of a working tag when no ammonia is present in the box (image extracted from Movie S1 in the SI). (C) Tag stops responding when ammonia is present, and the smartphone can no longer detect the NFC tag (image extracted from Movie S1).

As a reader, we used an NFC enabled smartphone (HUAWEI P9) to probe the tag. With the NFC tag modified with PEGS, we monitored the presence of NH_3 in a sealed box wirelessly, to simulate a food package that contains a decaying food. In this configuration, if no ammonia gas is present inside the box, the reader (i.e., smartphone) can communicate with the tag as it receives enough power to turn on, indicating that there is no detectable gas in the box (Movie S1). However, the tag fails to communicate with the smartphone when 15 mL of 10% ammonia solution is injected into the box which indicates the presence of detectable amounts of gas inside the sealed environment. We can tailor the switching point, at which the communication is stopped, by changing the parallel resistor, depending on the application.

CONCLUSIONS

We presented an entirely new class of near-zero-cost, electrical, gas sensors that can quantitatively detect the level of water-soluble gases in the atmosphere, using cellulose paper as the sensing material. Among the gases we tested (i.e., CO, CO_2, H_2S, TMA, NH_3), PEGS were most sensitive to ammonia, because of its high solubility in water. PEGS exhibited comparable or better performance in terms of the lower limit of detection, response time, sensitivity and cross-sensitivity, than commercially available low-cost ammonia sensors, while requiring no heating or complex manufacturing processes/materials. PEGS are particularly suitable for operation at high RH (90%–100%), where many existing sensing technologies (e.g., metal-oxide semiconductor,[37,38] electrochemical)[39] cannot operate (optimally or at all). In fact, PEGS perform the best, in terms of sensitivity, at RH > 60%. In this work, PEGS were produced using a ballpoint pen and a robotic cutter plotter, although the devices can be produced using existing high-volume printing methods such as screen printing, inkjet, and roll-to-roll printing. PEGS are produced with environmentally friendly, nontoxic, and biodegradable materials (cellulose paper can dissociate in soil) and are suitable for incineration.

However, the PEGS technology has the following four disadvantages:

(i) PEGS are highly sensitive to RH; this can be overcome by using PEGS in applications where the RH remains constant (e.g., food packaging) or by monitoring RH with additional (dedicated) sensors to account for any fluctuations in RH.

(ii) PEGS have low-specificity (i.e., cross-sensitive to a range of gases). Even though this was not an issue for the experiments involving food monitoring, it may be for applications requiring the detection of a specific gas. For these cases, PEGS can be modified with various chemical additives to tune sensitivity to the target gas through liquid-phase chemical reactions.[40,41] The sensors modified can be operated as a sensor array, the response of which can be fed into a mathematical model to estimate the type and concentration of a gaseous analyte.

(iii) PEGS require moisture for operation; therefore, PEGS may not function with sufficiently high performance in environments with low RH (<20%) in its current form.

(iv) PEGS are not suitable for high-temperature applications, since they are constructed using organic materials.

We demonstrated the use of PEGS in monitoring gases in the headspace of packaged food items, namely, fillets of cod and chicken breast. We confirmed a clear correlation between the response of PEGS and microbial counts measured through microbiological cultures. Hence, PEGS are suitable for use as an indicator of change of freshness, because of microbial contamination in packaged meat. Comparison with the state-of-the-art micromachined metal oxide gas sensor-based electronic nose (see section SI–P3 and Figure S7 in the SI) further revealed that the PEGS technology offers levels of performance that can exceed existing, much more sophisti-

DOI: 10.1021/acssensors.9b00555
ACS Sens. 2019, 4, 1662–1669

cated, sensing technologies. Although we did not study in detail in this work, PEGS can sense the presence of vapors of water-miscible organic solvents such as acetone, which will be the topic of a future study (Figure S8 in the SI).

PEGS technology can be integrated into NFC tags to produce on/off-type wirelessly powered sensors that can also be interrogated wirelessly with a smartphone. In the future, this can be extended to produce quantitative sensors (instead of just on/off) that can be probed and powered wirelessly using next-generation disposable integrated circuits for NFC, containing elements with more mixed-signal functions. Although, in this work, we have primarily explored the use of PEGS in food packaging, its use is most certainly not limited to this application. PEGS can find uses in the chemical industry (where hazardous gases need to be monitored), medical analysis, farming, and environmental monitoring.[42]

EXPERIMENTAL SECTION

Sensor Fabrication. For the fabrication of the paper sensors, we mixed conductive carbon ink (No. C2130925D1, GWENT Group) in a ratio of 55/45 wt % with a diluent (No. S60118D3, GWENT Group). To fabricate the electrodes, we used a cutter plotter (GRAPHTEC, Model CE6000-40) and a ballpoint pen (Sakura Gelly Roll METALLIC) which we cleaned with acetone and manually filled with the mixture of carbon ink. The electrodes were printed on chromatography paper (WhatmanTM, grade 1 chromatography paper, 20 cm × 20 cm, 0.18 mm thickness) and dried at 60 °C for 30 min. We printed three fingers on each electrode with 1 mm spacing between each finger of the electrodes for the characterization experiments and 2 mm spacing for the food trials (see Figure S9 in the SI).

Sensor Characterization Setup. The homemade characterization setup consisted of a polytetrafluoroethylene (PTFE) chamber that measured 120 mm × 60 mm × 40 mm (= 288 cm^3). It had one inlet (6 mm diameter), which divided into three supply lines using a cross connector. A cotton pad supported mixing of the gases inside the cross connector. The gas supply was controlled by mass flow controllers (MFCs, type GM50A from MKS); two MFCs controlled the level of RH in the chamber using a humidified and dry stream of pure nitrogen and the third MFC provided the test gas (usually premixed to some ratio in nitrogen by the supplier). The nitrogen flow was humidified by bubbling through deionized water (Figure S10 in the SI). We purchased all gases from BOC with a C-level certificate (±) of analysis of 5%.

Monitoring Food Spoilage. A single experiment consisted of three plastic food containers (180 mL each), two with a sample of food (20−40 g of either chicken breast or cod fish) and one with a few milliliters of water to create 100% RH as control. Each container had two PEGS and one humidity sensor (Model HIH-5030) inside. We added 20 μL of deionized water to each paper sensor before the experiment. This allowed the sensor to reach equilibrium with the high humidity atmosphere inside the containers faster (usually within 4−6 h). We evaluated experimentally that with the addition of 20 μL of water, the water content of the sensors was close to the equilibrium water content at 100% RH. If this step was skipped, it took up to 15 h for the paper to reach equilibrium. During this time, information concerning spoilage gases could not be collected.

Electrical Measurements. We applied a sinusoidal voltage signal with an amplitude of 0.1−10 V to the sensor and used a transimpedance amplifier with gain resistors of 20 kΩ to 120 MΩ to amplify and read the output signal (current). We measured the amplitude of this signal, which corresponded to the magnitude |Z| of the impedance of the sensor. For the characterization of the sensors, we took a measurement every second, together with a measurement of humidity (from a commercial sensor, Model HIH-5030) inside the chamber. In the food spoilage experiments, a recording was made every minute.

Microbial Cultures. We prepared a sterilized brain heart infusion agar (BHIA) and added 20 mL of the mixture to 27 Petri dishes to create a growth medium. Every 24 h, we blended a solid food sample (cod/chicken 5 g) in a stomacher tool with physiological water in a ratio of 1/10. The resulting liquid was further diluted with physiological water to obtain three dilutions between 10^{-2} and 10^{-5}. For each dilution, we added 100 μL of the sample to the Petri dishes containing the growth medium and incubated at a constant temperature of 37 °C. After 24 h, we used an image processing software (ImageJ) to count the colonies on each Petri dish to estimate the level of microbial contamination.

ASSOCIATED CONTENT

Supporting Information

The Supporting Information is available free of charge on the ACS Publications website at DOI: 10.1021/acssensors.9b00555.

Further discussions on the accuracy of the model proposed in the main text (section SI−P1); the case of NH_3 and trimethylamine (section SI−P1.1); a model for predicting ionic conductivity (section SI−P1.2); data analysis of food spoilage experiments (section SI−P2); comparison with state-of-the-art electronic nose (section SI−P3); Figures S1−S14 (also see www.guderesearch.com) (PDF)

Movie (MP4)

AUTHOR INFORMATION

Corresponding Author

*E-mail: guder@imperial.ac.uk.

ORCID

Sina Naficy: 0000-0001-9168-6746

Andrea Ponzoni: 0000-0001-9955-5118

Firat Güder: 0000-0001-5454-0609

Funding

Financial support through EPSRC (No. EP/R010242/1) and EPSRC DTP (Reference No. 1846144) is acknolwedged.

Notes

The authors declare no competing financial interest.

ACKNOWLEDGMENTS

F.G. and G.B. would like to thank EPSRC (EP/R010242/1), General Electric Healthcare and Imperial College, Department of Bioengineering for their generous support. F.G. and M.G. thank Imperial College Centre for Plastic Electronics and Centre for Doctoral Training in Plastic Electronics. F.G. also acknowledges Agri Futures Lab. M.K. acknowledges EPSRC DTP (Reference: 1846144). M.S. and A.P. acknowledge Lombardia Region and Consiglio Nazionale delle Ricerche for funding through the project Future Home for Future Communities. S.N. acknowledges the Australian Endeavour Research Fellowship program for funding. We would like to thank Dr. Danny O'Hare and Dr. Alar Ainla for the fruitful discussions.

ABBREVIATIONS

PEGS, paper-based electrical gas sensor; RH, relative humidity; NFC, near-field communication; ADC, analog-to-digital converter; TVB-N, total-volatile-basic nitrogen; COV, coefficient of variance; DI, deionized; CFU, colony forming units; IC, integrated circuit; PTFE, polytetrafluoroethylene; MFC, mass-flow controller; BHIA, brain heart infusion agar

DOI: 10.1021/acssensors.9b00555
ACS Sens. 2019, 4, 1662−1669

REFERENCES

(1) Springmann, M.; Clark, M.; Mason-D'Croz, D.; Wiebe, K.; Bodirsky, B. L.; Lassaletta, L.; De Vries, W.; Vermeulen, S. J.; Herrero, M.; Carlson, K. M.; et al. Options for Keeping the Food System within Environmental Limits. *Nature* **2018**, *562* (7728), 519−525.

(2) *World Food and Agriculture—Statistical Pocketbook*; Food and Agriculture Organization of the United Nations: Rome, Italy, 2013.

(3) Fox, T.; Fimeche, C. *Global Food. Waste Not, Want Not*; Institution of Mechanical Engineers, 2013.

(4) Quested, T.; Ingle, R.; Parry, A. *Household Food and Drink Waste in the UK 2012*; Waste and Resources Action Programme (WRAP), 2013.

(5) Labuza, T. P.; Taoukis, P. S. The Relationship between Processing and Shelf-Life. In *Foods for the '90s*; Birch, G., Campell-Plat, G., Lindley, M., Eds.; Elsevier Applied Science: New York, 1990; pp 73−106.

(6) Koutsodendris, A.; Papatheodorou, G.; Kougiourouki, O.; Georgiadis, M. Benthic Marine Litter in Four Gulfs in Greece, Eastern Mediterranean; Abundance, Composition and Source Identification. *Estuarine, Coastal Shelf Sci.* **2008**, *77* (3), 501−512.

(7) Yam, K. L.; Takhistov, P. T.; Miltz, J. Intelligent Packaging: Concepts and Applications. *J. Food Sci.* **2005**, *70* (1), R1−R10.

(8) De Jong, A. R.; Boumans, H.; Slaghek, T.; Van Veen, J.; Rijk, R.; Van Zandvoort, M. Active and Intelligent Packaging for Food: Is It the Future? *Food Addit. Contam.* **2005**, *22* (10), 975−979.

(9) Yam, K. L. Intelligent Packaging to Enhance Food Safety and Quality. In *Emerging Food Packaging Technologies*; Yam, K. L., Lee, D. S., Eds.; Woodhead Publishing, 2012; pp 137−152 (DOI: 10.1533/9780857095664.2.137).

(10) Liu, S. F.; Petty, A. R.; Sazama, G. T.; Swager, T. M. Single-Walled Carbon Nanotube/Metalloporphyrin Composites for the Chemiresistive Detection of Amines and Meat Spoilage. *Angew. Chem., Int. Ed.* **2015**, *54* (22), 6554−6557.

(11) Alur, M. D.; Doke, S. N.; Warrier, S. B.; Nair, P. M. Biochemical Methods for Determination of Spoilage of Foods of Animal Origin: A Critical Evaluation. *J. Food Sci. Technol.* **1995**, *32* (3), 181−188.

(12) Taoukis, P. S.; Koutsoumanis, K.; Nychas, G. J. E. Use of Time-Temperature Integrators and Predictive Modelling for Shelf Life Control of Chilled Fish under Dynamic Storage Conditions. *Int. J. Food Microbiol.* **1999**, *53* (1), 21−31.

(13) Venugopal, V. Biosensors in Fish Production and Quality Control. *Biosens. Bioelectron.* **2002**, *17*, 147−157.

(14) Dalgaard, P.; Buch, P.; Silberg, S. Seafood Spoilage Predictor - Development and Distribution of a Product Specific Application Software. *Int. J. Food Microbiol.* **2002**, *73* (2−3), 343−349.

(15) Mills, A. Oxygen Indicators and Intelligent Inks for Packaging Food. In *Chemical Society Reviews*; Royal Society of Chemistry, 2005; pp 1003−1011 (DOI: 10.1039/b503997p).

(16) Giannakourou, M. C.; Koutsoumanis, K.; Nychas, G. J. E.; Taoukis, P. S. Field Evaluation of the Application of Time Temperature Integrators for Monitoring Fish Quality in the Chill Chain. *Int. J. Food Microbiol.* **2005**, *102* (3), 323−336.

(17) Pacquit, A.; Frisby, J.; Diamond, D.; Lau, K. T.; Farrell, A.; Quilty, B.; Diamond, D. Development of a Smart Packaging for the Monitoring of Fish Spoilage. *Food Chem.* **2007**, *102* (2), 466−470.

(18) Dainelli, D.; Gontard, N.; Spyropoulos, D.; Zondervan-van den Beuken, E.; Tobback, P. Active and Intelligent Food Packaging: Legal Aspects and Safety Concerns. *Trends Food Sci. Technol.* **2008**, *19*, S103−S112.

(19) Lau, O.-W.; Wong, S.-K. Contamination in Food from Packaging Material. *J. Chromatogr. A* **2000**, *882*, 255−270.

(20) Mirica, K. A.; Weis, J. G.; Schnorr, J. M.; Esser, B.; Swager, T. M. Mechanical Drawing of Gas Sensors on Paper. *Angew. Chem.* **2012**, *124* (43), 10898−10903.

(21) Güder, F.; Ainla, A.; Redston, J.; Mosadegh, B.; Glavan, A.; Martin, T. J.; Whitesides, G. M. Paper-Based Electrical Respiration Sensor. *Angew. Chem.* **2016**, *128* (19), 5821−5826.

(22) Alkin, K.; Stockinger, T.; Zirkl, M.; Stadlober, B.; Bauer-Gogonea, S.; Kaltenbrunner, M.; Bauer, S.; Müller, U.; Schwödiauer, R. Paper-Based Printed Impedance Sensors for Water Sorption and Humidity Analysis. *Flex. Print. Electron.* **2017**, *2*, 014005.

(23) Fazzalari, F. A. Compilation of Odor and Taste Threshold Values Data. In *ASTM Data Service*; ASTM, 1978 (DOI: 10.1520/DS48A-EB).

(24) Leonardos, G.; Kendall, D.; Barnard, N. Odor Threshold Determinations of 53 Odorant Chemicals. *J. Air Pollut. Control Assoc.* **1969**, *19* (2), 91−95.

(25) Erickson, R. J. An Evaluation of Mathematical Models for the Effects of PH and Temperature on Ammonia Toxicity to Aquatic Organisms. *Water Res.* **1985**, *19* (8), 1047−1058.

(26) Kuen, C. *Determination of the Moisture Sorption Curves of Cellulose for Transformers Depending on the Degree of Polymerization*; TU Graz, 2008.

(27) Glasstone, S. Dispersion of Conductance at High Frequencies. In *Introduction to Electrochemistry*; Van Nostrand, D., Ed.; Maurice Press: New York, 2012; p 101.

(28) The coefficient of variation is defined as the ratio of the standard deviation to the mean.

(29) Lide, D. R. *CRC Handbook of Chemistry and Physics*, 89th Edition (Internet Version 2009); CRC Press: Boca Raton, FL, 2009.

(30) Hales, J. M.; Drewes, D. R. Solubility of Ammonia in Water at Low Concentrations. *Atmos. Environ.* **1979**, *13* (8), 1133−1147.

(31) Botta, J. R.; Lauder, J. T.; Jewer, M. A. Effect of Methodology on Total Volatile Basic Nitrogen (TVB−N) Determination as an Index of Quality of Fresh Atlantic Cod (Gadus Morhua). *J. Food Sci.* **1984**, *49* (3), 734−736.

(32) Henry's Law: "Amount of dissolved gas is proportional to its partial pressure in the gas phase with the proportionality factor called Henry's Law constant."

(33) Heising, J. K.; Bartels, P. V.; Van Boekel, M. A. J. S.; Dekker, M. Non-Destructive Sensing of the Freshness of Packed Cod Fish Using Conductivity and PH Electrodes. *J. Food Eng.* **2014**, *124*, 80−85.

(34) International Commission on Microbiological Specifications for Food. *Microorganisms in Foods 7—Microbiological Testing in Food Safety and Management*; Springer: New York, 2018.

(35) *Guidelines for Assessing the Microbiological Safety of Ready-to-Eat Foods*; Health Protection Agency: London, 2009.

(36) Azzarelli, J. M.; Mirica, K. A.; Ravnsbæk, J. B.; Swager, T. M. Wireless Gas Detection with a Smartphone via Rf Communication. *Proc. Natl. Acad. Sci. U. S. A.* **2014**, *111* (51), 18162−18166.

(37) Güder, F.; Yang, Y.; Menzel, A.; Wang, C.; Danhof, J.; Subannajui, K.; Hartel, A.; Hiller, D.; Kozhummal, R.; Ramgir, N. S.; Cimalla, V.; Schwarz, U. T.; Zacharias, M.; et al. Superior Functionality by Design: Selective Ozone Sensing Realized by Rationally Constructed High-Index ZnO Surfaces. *Small* **2012**, *8* (21), 3307−3314.

(38) Wongchoosuk, C.; Subannajui, K.; Wang, C.; Yang, Y.; Güder, F.; Kerdcharoen, T.; Cimalla, V.; Zacharias, M. Electronic Nose for Toxic Gas Detection Based on Photostimulated Core−shell Nanowires. *RSC Adv.* **2014**, *4* (66), 35084−35088.

(39) Rahman, M. M.; Asiri, A. M. *Electrochemical Sensors Technology*; Rahman, M. M., Asiri, A. M., Eds.; InTech, 2017 (DOI: 10.5772/65230).

(40) Rakow, N. A.; Suslick, K. S. A Colorimetric Sensor Array for Odour Visualization. *Nature* **2000**, *406* (6797), 710−713.

(41) Dickinson, T. A.; White, J.; Kauer, J. S.; Walt, D. R. A Chemical-Detecting System Based on a Cross-Reactive Optical Sensor Array. *Nature* **1996**, *382* (6593), 697−700.

(42) Timmer, B.; Olthuis, W.; van den Berg, A. Ammonia Sensors and Their Applications—A Review. *Sens. Actuators, B* **2005**, *107*, 666−677.

DOI: 10.1021/acssensors.9b00555
ACS Sens. 2019, 4, 1662−1669